Tryptophan 80 and Leucine 143 Are Critical for the Hydride Transfer Step of Thymidylate Synthase by Controlling Active Site Access[†,‡]

Timothy A. Fritz,[§] Lu Liu, Janet S. Finer-Moore, and Robert M. Stroud*

Macromolecular Structure Group, Department of Biochemistry and Biophysics and Department of Pharmaceutical Chemistry, The University of California−San Francisco, San Francisco, California 94143-0448

Received November 30, 2001; Revised Manuscript Received March 7, 2002

ABSTRACT: Mutant forms of thymidylate synthase (TS) with substitutions at the conserved active site residue, Trp 80, are deficient in the hydride transfer step of the TS reaction. These mutants produce a β-mercaptoethanol (β-ME) adduct of the 2′-deoxyuridine-5′-monophosphate (dUMP) exocyclic methylene intermediate. Trp 80 has been proposed to assist hydride transfer by stabilizing a 5,6,7,8-tetrahydrofolate (THF) radical cation intermediate [Barrett, J. E., Lucero, C. M., and Schultz, P. G. (1999) *J. Am. Chem. Soc. 121*, 7965−7966.] formed after THF changes its binding from the cofactor pocket to a putative alternate site. To understand the molecular basis of hydride transfer deficiency in a mutant in which Trp 80 was changed to Gly, we determined the X-ray structures of this mutant *Escherichia coli* TS complexed with dUMP and the folate analogue 10-propargyl-5,8-dideazafolate (CB3717) and of the wild-type enzyme complexed with dUMP and THF. The mutant enzyme has a cavity in the active site continuous with bulk solvent. This cavity, sealed from bulk solvent in wild-type TS by Leu 143, would allow nucleophilic attack of β-ME on the dUMP C5 exocyclic methylene. The structure of the wild-type enzyme/dUMP/THF complex shows that THF is bound in the cofactor binding pocket and is well positioned to transfer hydride to the dUMP exocyclic methylene. Together, these results suggest that THF does not reorient during hydride transfer and indicate that the role of Trp 80 may be to orient Leu 143 to shield the active site from bulk solvent and to optimally position the cofactor for hydride transfer.

Thymidylate synthase (TS)[1] catalyzes the conversion of the substrate 2′-deoxyuridine-5′-monophosphate (dUMP) to the DNA precursor deoxythymidine-5′-monophosphate (dTMP) using the cofactor (6*R*)-5,10-methylene-5,6,7,8-tetrahydrofolate (mTHF) as both the methyl donor and the reductant. The reaction mechanism has been extensively characterized both biochemically and structurally (*1*−*3*) and begins with the enzyme enclosing the substrate and cofactor in a process termed segmental accommodation (*4*). The reaction proceeds by Michael addition of the catalytic cysteine, Cys 146,[2] to C6 of dUMP (Scheme 1, **I**). This activates the C5 of dUMP for attack on the N5 iminium ion of mTHF (Scheme 1, **II**) and leads to the formation of a ternary complex in which both dUMP and mTHF are covalently bound to the enzyme (Scheme 1, **III**). Abstraction of a proton from C5 of dUMP assisted by an active site tyrosine residue (*5*) leads to the breakdown of the ternary complex and the formation of the intermediates THF and dUMP containing a C5 exocyclic methylene group (Scheme 1, **V**). In the final and least understood step of the reaction mechanism, the THF C6 hydride reduces the dUMP C5 exocyclic methylene to form the products dTMP and 7,8-dihydrofolate (Scheme 1, process A).

Until recently, direct evidence for the existence of the dUMP C5 exocyclic methylene was lacking. An investigation into the function of the conserved active site residue Trp 80 led to the discovery of an unexpected product formed by mutants containing unnatural amino acids substituted for this residue (*6*). Characterization of the unusual product showed it to be 5-(2-hydroxyethyl)thiomethyl-dUMP (HETM-dUMP), the β-ME adduct of the dUMP exocyclic methylene. Thus, in these mutants, β-ME adds to the dUMP exocyclic methylene instead of the normal THF C6 hydride (Scheme 1, process B). The source of the β-ME is the TS reaction buffer, which contains 70 mM of the thiol to protect the catalytic cysteine residue from oxidation. On the basis of their studies showing a correlation between the theoretical ability of residue 80 to bind Na^+ and the k_{cat} of the enzyme, Barrett et al. (*7*) proposed a mechanism of hydride transfer in which Trp 80 stabilizes a cationic THF radical intermediate generated during the reaction. In this model, the THF

[†] This work was supported by a USPHS grant, NIH Grant CA-41323 (J.F.-M.). T.A.F. was supported by a NRSA Postdoctoral Fellowship AI-10279 and a UCSF Herbert W. Boyer Postdoctoral Fellowship.

[‡] The coordinates and structure factors for the structures presented in this paper have been deposited with the RCSB Protein Data Bank under entries 1KZI (EcTS/dUMP/THF) and 1KZJ (W80G-EcTS/dUMP/CB3717).

* To whom correspondence should be addressed. Phone: 415-476-4224. Fax: 415-476-1902. E-mail: stroud@msg.ucsf.edu.

[§] Present address: National Institute of Diabetes and Digestive and Kidney Diseases, 9000 Rockville Pike, Bethesda, MD 20892.

[1] Abbreviations: TS, thymidylate synthase; EcTS, *Escherichia coli* TS; LcTS, *Lactobacillus casei* TS; mTHF, (6*R*)-5,10-methylene-5,6,7,8-tetrahydrofolate; THF, (6*S*)-5,6,7,8-tetrahydrofolate; DHF, 7,8-dihydrofolate; dUMP, 2′-deoxyuridine-5′-monophosphate; HETM-dUMP, 5-(2-hydroxyethyl)thiomethyl-dUMP; FdUMP, 5-fluoro-dUMP; dTMP, 2′-deoxythymidine-5′-monophosphate; CB3717, 10-propargyl-5,8-dideazafolate; β-ME, β-mercaptoethanol; DTT, dithiothreitol.

[2] Unless otherwise noted, the numbering system of *Escherichia coli* TS is used.

10.1021/bi012108c CCC: $22.00
Published on Web 05/09/2002

Scheme 1

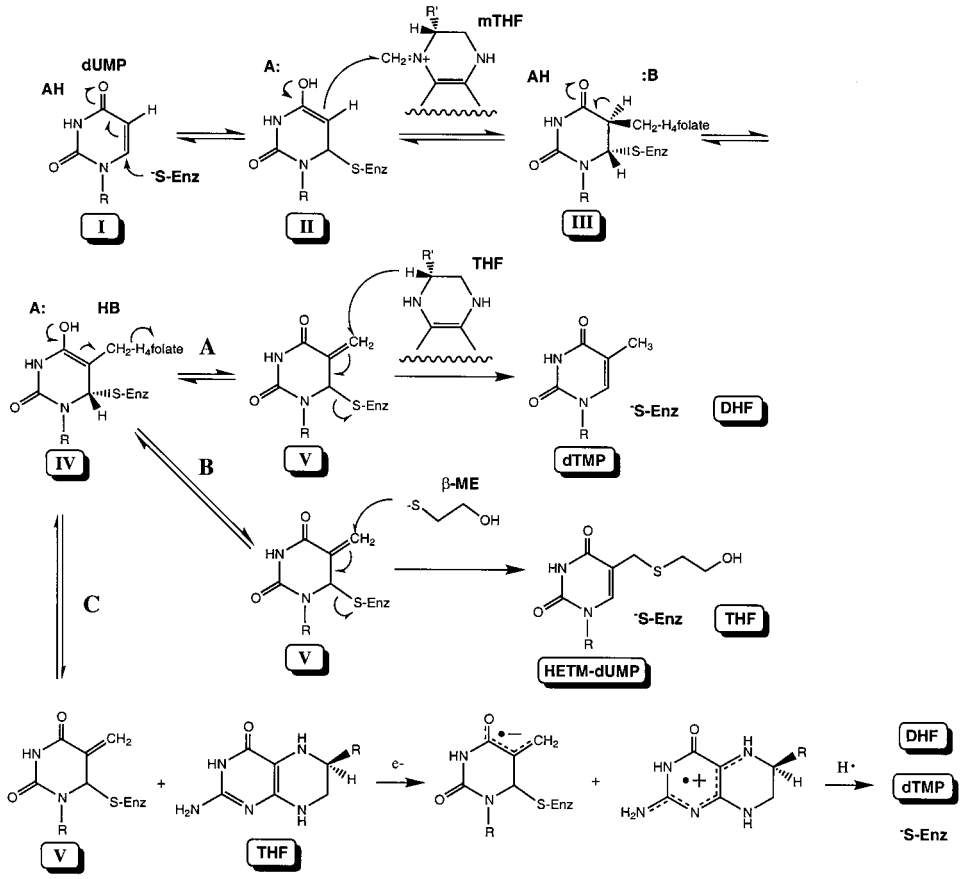

produced after breakdown of the covalent ternary complex shifts to a putative alternative binding position in the active site. This alternative site was revealed by the X-ray crystallographic structure of the antifolate BW1843U89 bound to EcTS (*8*, *9*). The reduction of the dUMP exocyclic methylene was then proposed to occur in two stages (*7*, *10*). First, a single electron is transferred from the reoriented THF to the dUMP exocyclic methylene, generating a THF radical cation and a dUMP exocyclic methylene radical anion (Scheme 1, process C). Then, the THF radical cation moves back to its original location to transfer the remaining electron and proton to the dUMP exocyclic methylene radical anion to complete the reduction. It was argued that the shift in THF position to the alternative site would enable the THF radical cation to be stabilized by the π electrons of Trp 80 and those of the uracil ring (*7*).

To learn how THF binds to the EcTS active site and to understand the reason for the hydride transfer deficiency of a Trp 80 mutant, we determined the crystal structure of wild-type EcTS bound to dUMP and THF and, for comparison, the structure of the W80G-EcTS mutant bound to dUMP and the folate analogue CB3717. The structure of the wild-type enzyme complexed with dUMP and THF clearly shows that THF does not bind in the alternative site. Rather, THF is bound within the known cofactor site and is ideally positioned to donate its C6 hydride to the exocyclic methylene. The structure of the mutant enzyme reveals a large cavity in the active site that is sufficient to accommodate β-ME and allows it access to C5 of dUMP. The cavity is open to bulk solvent because of a failure of the side chain of Leu 143 to reorient upon ternary complex formation. These results suggest that the role of Trp 80 may not be the electronic stabilization of a THF radical cation reaction intermediate but rather it is proper orientation of Leu 143 and the cofactor for efficient hydride transfer.

MATERIALS AND METHODS

W80G Mutant Creation and Characterization. Site-directed mutagenesis of *E. coli* Thy A was performed using the QuickChange site-directed mutagenesis kit (Stratagene, La Jolla, CA) using the oligonucleotide CGAAAACAATGTCACCATC*GGT*GACGAATGGGCCGATG and its complement. The plasmid was expressed in *E. coli* strain χ2913-(DE3). Reaction mixtures (0.5 mL) containing 250 mM dUMP and varying concentrations of (6*R*)-CH_2H_4 folate in TES buffer (50 mM TES, 25 mM $MgCl_2$, 6.5 mM formaldehyde, 1 mM EDTA, 75 mM β-ME, pH 7.4) and 1 mM W80G-EcTS were incubated for 60 min. Reactions were quenched by the addition of 30 mL of 20% (w/v) trichloroacetic acid to precipitate the protein. Products (dUMP and HETM-dUMP) were quantified as described (*11*).

Protein Purification and Crystallization. Wild-type EcTS was expressed and purified as described previously (*12*). The W80G mutant was similarly purified but required an additional purification step that consisted of binding the enzyme to a Poros HQ column (Perseptive Biosystems) in 50 mM Tris (pH 8.0) and elution using a 0−1.0 M NaCl gradient. Wild-type and mutant EcTS were stored at −20 °C in 85% saturated ammonium sulfate and were dialyzed at 4 °C against 5 mM Tris (pH 8), 5 mM dithiothreitol (DTT), and 1 mM EDTA before crystallization.

Crystals were grown by the hanging drop vapor diffusion method over 1 mL of well buffer. For the wild-type enzyme, drops were formed by mixing 2.5 μL of a protein solution containing 6.1 mg/mL EcTS, 2 mM THF, 1 mM dUMP, 5 mM DTT, and 0.9 mM EDTA with 2.5 μL of a well buffer containing 100 mM TAPS buffer (pH 8.6), 2.6 M $(NH_4)_2SO_4$, and 10 mM DTT. Crystals of W80G-EcTS were grown in 5 mL drops created by mixing 2.5 μL of a protein solution containing 3−5 mg/mL enzyme, 2 mM dUMP, 1 mM CB3717, and 5 mM DTT with 2.5 μL of a well buffer containing 0.1 M Tris (pH 8.5), 22−26% (w/v) PEG 4000, 0.2 M sodium acetate, and 10 mM DTT.

Wild-type crystals were transferred to a solution of 0.1 M TAPS (pH 8.6), 2.7 M $(NH_4)_2SO_4$, 10 mM DTT, and 20% (v/v) glycerol for 15−30 s before cooling in a nitrogen cryostream. W80G crystals were briefly (15−30 s) placed in a solution containing 28% (w/v) PEG 4000, 0.1 M Tris (pH 8.5), 0.2 M sodium acetate, 10 mM DTT, and 15% (v/v) ethylene glycol before cooling. Diffraction intensities from single crystals were collected using 1.0° oscillations. Data for the W80G-EcTS complex were collected on beamline 7-1 at the Stanford Synchrotron Radiation Laboratory, while wild-type data were collected on an Raxis-IV detector using a rotating anode generator equipped with Osmic mirrors. Intensities from 180 (W80G) or 90 (wild-type) frames were integrated and scaled using the programs DENZO and SCALEPACK (*13*).

Structure Solution and Refinement. Structures were solved by molecular replacement using the reported ternary complex structure of EcTS/dUMP/ZD1694 (*14*) with the ligands and water omitted from the model. The wild-type EcTS/dUMP/THF structure was solved using the program AmoRe (*15*), and the W80G-EcTS/dUMP/CB3717 structure was solved using the program EPMR (*16*). Ligands were modeled into the electron density using the program XtalView (*17*). Structures were refined using simulated annealing (to remove model bias) followed by repeated cycles of conjugate gradient and B-factor minimization using the program CNS (*18*) and manual rebuilding using XtalView. The crystallographic data and refinement statistics are shown in Table 1.

Structure Analysis. Least-squares alignment of molecules and calculation of atomic rms deviations were done using the program LSQMAN. Computation of cavity and residue volumes was done using the program Voidoo (*19*). For cavity calculations, the probe radius (1.1 Å) was chosen to give a reasonable estimate of the cavity volume of the wild-type EcTS/dUMP/THF structure. Mutant cavity volumes were calculated after torsioning leucine 143 into its position adopted in the wild-type EcTS/dUMP/THF complex to seal the cavity from bulk solvent. Ligand−protein contacts were computed using the program Ligplot (*20*) and the LPC software (*21*). Figures 1, 3, and 5−7 were created using Swiss PDB Viewer (*22*) and POVray.

Table 1: Crystallographic Data and Refinement Statistics with Statistics for the Outer Resolution Shell Given in Parentheses

	WT/dUMP/THF	W80G/dUMP/CB3717
resoln (Å)	29.46−1.75	25.35−2.6
resoln, outer shell (Å)	1.81−1.75	2.69−2.60
a (Å)	125.3	95.5
b (Å)	125.3	84.6
c (Å)	66.8	111.5
β (deg)		111.4
space group	$P6_3$	$P2_1$
dimers/asymmetric unit	1	3
observed reflns	492 649	444 846
unique reflns	59 657	51 013
average $I/\sigma(I)$	32.0 (2.0)	8.9 (2.4)
completeness (%)	98.6 (88.1)	98.1 (92.4)
R_{merge} (%)	4.3 (45.4)	12.4 (41.0)
R_{work} (%)	19.7 (39.1)	21.5 (28.0)
R_{free} (%)	22.1 (42.0)	25.8 (34.0)
rmsd bonds (Å)	0.007	0.008
rmsd angles (deg)	1.5	1.5
rmsd dihedrals (deg)	24.1	24.6
mean B factor (Å^2)	27.3	20.8
total atoms	4805	13 460
water molecules	360	291

RESULTS

THF and dUMP Binding to Wild-Type EcTS. The EcTS/dUMP/THF structure crystallizes as a physiological homodimer in the asymmetric unit. A difference electron density map ($(F_o - F_c)\alpha_c$) calculated following molecular replacement showed density for THF and dUMP in both active sites. The final refined structure showed excellent density for both THF and dUMP in one active site while density for THF in the second active site was slightly broken, suggesting incomplete occupancy (Figure 1). Both protomers are in the closed conformation, and the electron density indicated the presence of a covalent bond between each catalytic cysteine (Cys 146) and the C6 atom of the corresponding dUMP molecule. Cysteine 192 of protomer **A** is derivatized with a molecule of dithiothreitol (DTT). This modification is accommodated by a simple reordering of the side chain of a surface lysine (Lys 120) and does not disrupt the primary fold of the protein. An additional cyclic, oxidized DTT molecule was indicated by electron density and modeled into the structure. Three carbonate ions and a molecule of glycerol were also revealed by electron density and modeled into the structure. Since each protomer is very similar to the other (C_α carbon rms deviation is 0.39 Å), the structure of only protomer **A** will be discussed.

The pterin group of THF contains one less ring compared to the 2-desamino-2-methylbenzoquinazoline moiety of the antifolate BW1843U89 (Figure 2). The crystal structure of the EcTS/dUMP/BW1843U89 complex (*8*, *9*) revealed that rings A and B of BW1843U89 bind to EcTS in nearly the same location as the pterin ring of the natural cofactor mTHF (*23*). However, the larger space occupied by the BW1843U89 suggested an alternative binding site for the two-ring pterin moiety of the cofactor (or THF) in which the pterin group might bind in the position occupied by rings B and C of BW1843U89. Binding of THF in this alternative site has been proposed because it was argued that this orientation would facilitate the hydride transfer step of the TS reaction mechanism (*7*).

The crystal structure of THF and dUMP bound to wild-type EcTS is shown in Figure 3A together with the proposed orientation of THF in the alternative site (*7*). Clearly, THF does not occupy the alternative binding site. Instead, it binds in essentially the same position as the cofactor mTHF (Figure 3B). Indeed, the hydrogen bonds and van der Waals interactions formed between the protein and THF are essentially the same as those between the protein and mTHF

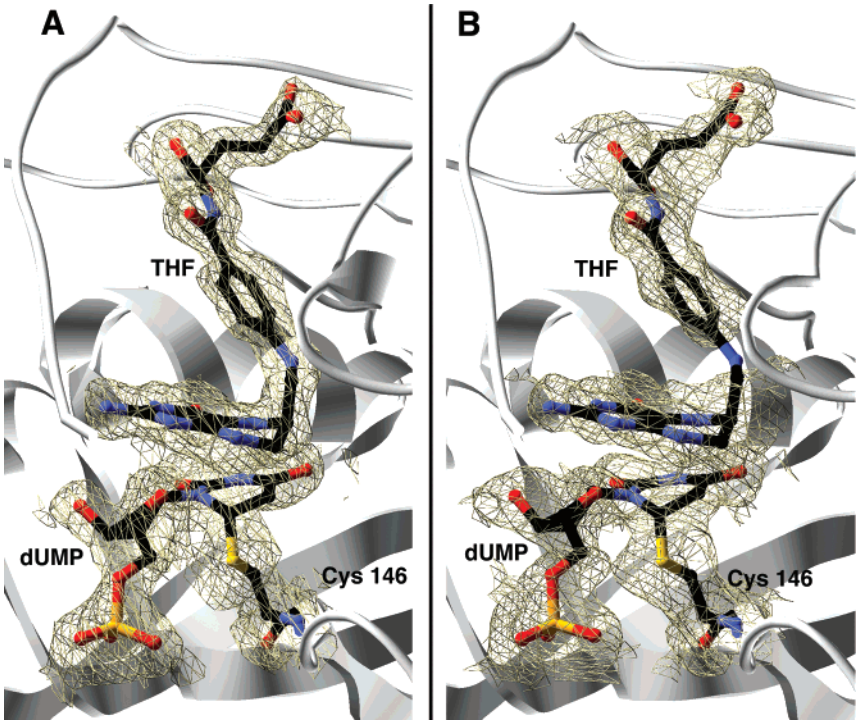

FIGURE 1: Electron density for THF, dUMP, and Cys 146 is well defined in each active site of the TS dimer. Simulated-annealing omit electron density maps (contoured at 2.5σ) were calculated from the final refined structure after omitting THF, dUMP, and Cys 146 first from the active site of protomer **A** (panel A) and then from the active site of protomer **B** (panel B).

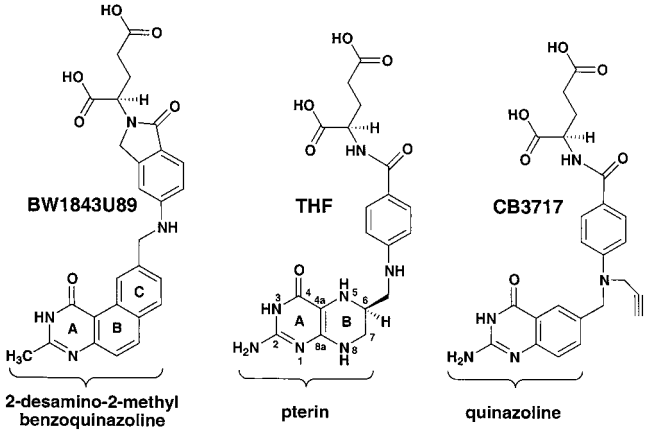

FIGURE 2: Chemical structures of the TS inhibitor BW1843U89, the TS reaction intermediate THF, and the folate analogue CB3717. The three-ring structure of the 2-desamino-2-methylbenzoquinazoline moiety of BW1843U89 and the two-ring structures of the pterin group of THF and the quinazoline moiety of CB3717 are indicated by the braces. Atom numbering for the pterin ring is shown.

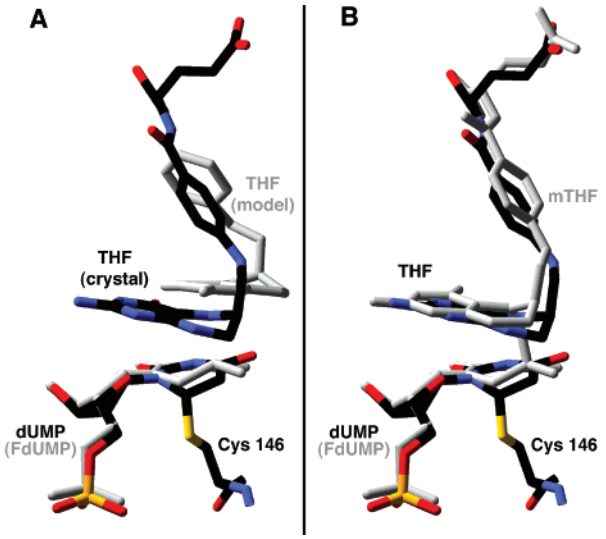

FIGURE 3: THF does not bind to the alternative site. (A) The orientations THF, dUMP, and Cys 146 (various colors) from the X-ray crystal structure are compared to the modeled orientation (*7*) of THF (gray) in the EcTS/FdUMP/mTHF structure (*23*). FdUMP (gray) from the EcTS/FdUMP/mTHF structure is also shown, but Cys 146 has been omitted for clarity. (B) The orientations of THF and dUMP (various colors) from the EcTS/dUMP/THF structure are compared to the orientations of mTHF and FdUMP (gray) from the EcTS/FdUMP/mTHF structure. Cys 146 is shown for the EcTS/dUMP/THF complex but has been omitted from the EcTS/FdUMP/mTHF complex for clarity. The overlapped pterin ring of THF obscures the mTHF methylene group, which is covalently bonded to C5 of FdUMP and N5 of mTHF.

(Figure 4). The overall rms deviation of C_α positions between protomer **A** of the EcTS/dUMP/THF structure and the EcTS/FdUMP/mTHF structure (which contains a protomer in the asymmetric unit) is 0.38 Å. A new water molecule (water 658) not observed in the EcTS/FdUMP/mTHF structure is seen in the active site of the EcTS/dUMP/THF complex (Figure 4A). This water molecule lies 3.8 Å from, and is directly in line with, the THF N5 atom.

CB3717 and dUMP Binding to W80G-EcTS. The log(k_{cat}) values for a series of unnatural amino acid variants of Trp 82 in *Lactobacillus casei* TS (EcTS Trp 80) correlated well with the theoretical binding energy of Na^+ to the π systems of the substituted side chains (*7*). These data indicate a role for Trp 80 in π electron stabilization of a positive charge on the cofactor during hydride transfer. Data showing that the most active variants of Trp 82 in LcTS are aromatic residues (*24*) also support such a role. However, π interactions of Trp 80 with THF are not essential for hydride transfer because, of eight mutants of Trp 82 tested in LcTS, several

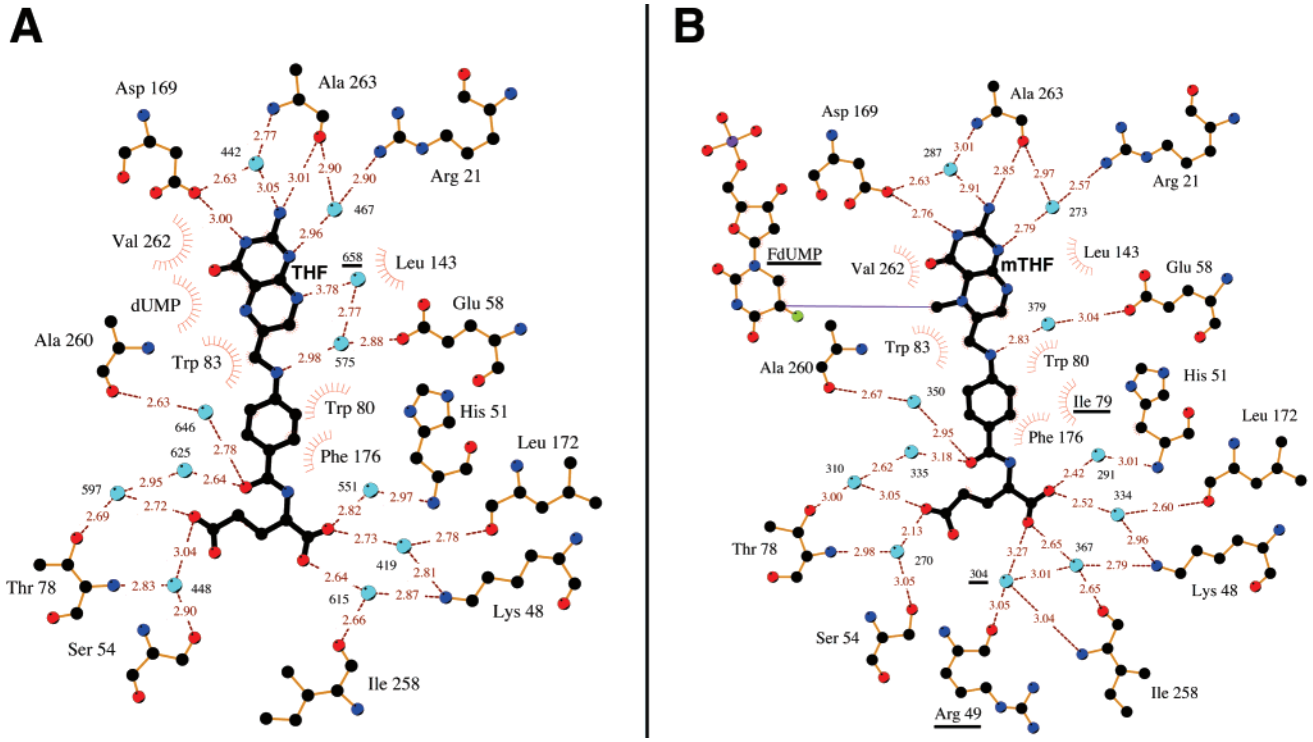

FIGURE 4: Binding of THF (A) and mTHF (B) to EcTS is nearly identical. Differences between the interactions of THF and mTHF with EcTS are underlined. Waters are shown in cyan, hydrogen bonds are shown as brown dashed lines together with the hydrogen bond distance, and hydrophobic interactions are shown as brown "eyelashes". The figure was generated using the program Ligplot (*20*).

nonaromatic variants are also active (*24*). To discover the requirements for catalysis of hydride transfer in TS, we therefore focused on the inactive mutant W80G. The EcTS W80G mutant produces nearly exclusively HETM-dUMP with no detectable levels of dTMP (data not shown). Thus, the W80G-EcTS mutant is a good model for understanding the hydride transfer step of the TS reaction because it catalyzes the formation of the dUMP C5 exocyclic methylene but is unable to carry out the subsequent reduction of the exocyclic methylene. Because of the low activity of this mutant, kinetic characterization of the enzyme was not possible, and we were unable to grow crystals of the mutant complexed with dUMP and THF.

To understand why the EcTS W80G mutant fails to reduce the exocyclic methylene, we determined the crystal structure of the W80G-EcTS/dUMP/CB3717 complex. CB3717's similarity to THF (Figure 2) makes it a good substitute for the cofactor intermediate. The complex crystallizes with three TS dimers in the asymmetric unit (Table 1). Dimers **1**, **2**, and **3** are composed of protomers **A** and **B**, **C** and **D**, and **E** and **F**, respectively, and each protomer active site is occupied by both dUMP and CB3717. dUMP is covalently bound to the catalytic cysteine in protomers **A**, **B**, **C**, and **F**. These four protomers are in the typical closed ternary complex conformation (*4*). Protomers **D** and **E** have a more open active site, and dUMP in these two protomers is not covalently bound to the active site cysteine. Dimers **1** and **2** are structurally similar with an rms deviation based on aligned C_α positions of 0.38 Å. The rms deviation between dimers **2** and **3** is 0.43 Å and that between dimers **1** and **3** is 0.54 Å. Protomer **E** has the most open active site and the highest ligand B factors of the six protomers. Electron density was absent for the three carboxyl terminal residues of protomer **E**, so these were removed from the final structure.

The orientations of the ligands in each protomer of the W80G-EcTS/dUMP/CB3717 crystal structure are the same within experimental error and are remarkably similar to that of the corresponding wild-type enzyme (Figure 5). All of the protein−ligand contacts between the enzyme and dUMP are preserved between the two structures. CB3717 interacts with nine residues of the wild-type enzyme, and all of these interactions except for those to Trp 80 (the residue that was mutated to glycine) and Leu 143 have been preserved in the mutant complex. Hydrophobic contacts to CB3717 by the Trp 80 side chain of the wild-type enzyme are replaced by less favorable interactions with solvent (waters 656 and 657).

Active Site Accessibility. The loss of the Trp 80 side chain leads to the expansion of an active site cavity occupied by water molecules in the wild-type EcTS/dUMP/CB3717 and wild-type EcTS/dUMP/THF structures (Figure 6). The cavity is observed in each of the six active sites. The cavity volumes of the mutant structures range from 258 $Å^3$ (protomer **C**) to 572 $Å^3$ (protomer **D**), while that of the wild-type structure is 89 $Å^3$. The volume of the cavity in the active site of protomer **E** cannot be calculated because the three carboxyl terminal residues, which form a wall of the cavity, are disordered. In the mutant, the cavity is easily large enough to accommodate a molecule of β-ME and allows ready access to the C5 atom of dUMP, while in the wild-type enzyme the volume of the cavity is not sufficient to accommodate a β-ME molecule. The environment of the newly created portion of the cavity is largely nonpolar, being surrounded by the side chains of residues Trp 61, Ile 69, Leu 72, Ile 79, Trp 83, Leu 90, and Leu 143. Such a cavity would form a good environment for the relatively nonpolar β-ME molecule. In wild-type EcTS, Trp 83 and Leu 143 reorient as cofactor binds, maximizing hydrophobic contacts with the pterin ring and blocking access to this cavity. In W80G-EcTS, Leu 143

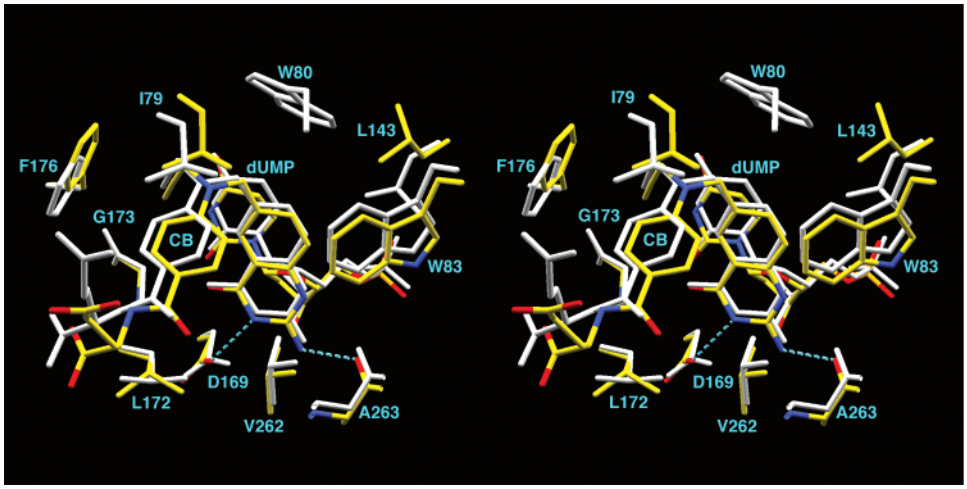

FIGURE 5: Binding of CB3717 to the EcTS W80G mutant is the same as to the wild-type enzyme. The divergent stereoview shows the interactions of CB3717 with active site residues in the EcTS W80G mutant (various colors) or to the wild-type enzyme (gray). Hydrogen bonds are shown by the dashed lines. The structure of the wild-type EcTS/dUMP/CB3717 complex (protomer **A**) is from the RCSB Protein Data Bank (entry 1KCE) and was aligned with the active site of protomer **A** of the W80G-EcTS/dUMP/CB3717 structure using the program LSQMAN (*36*).

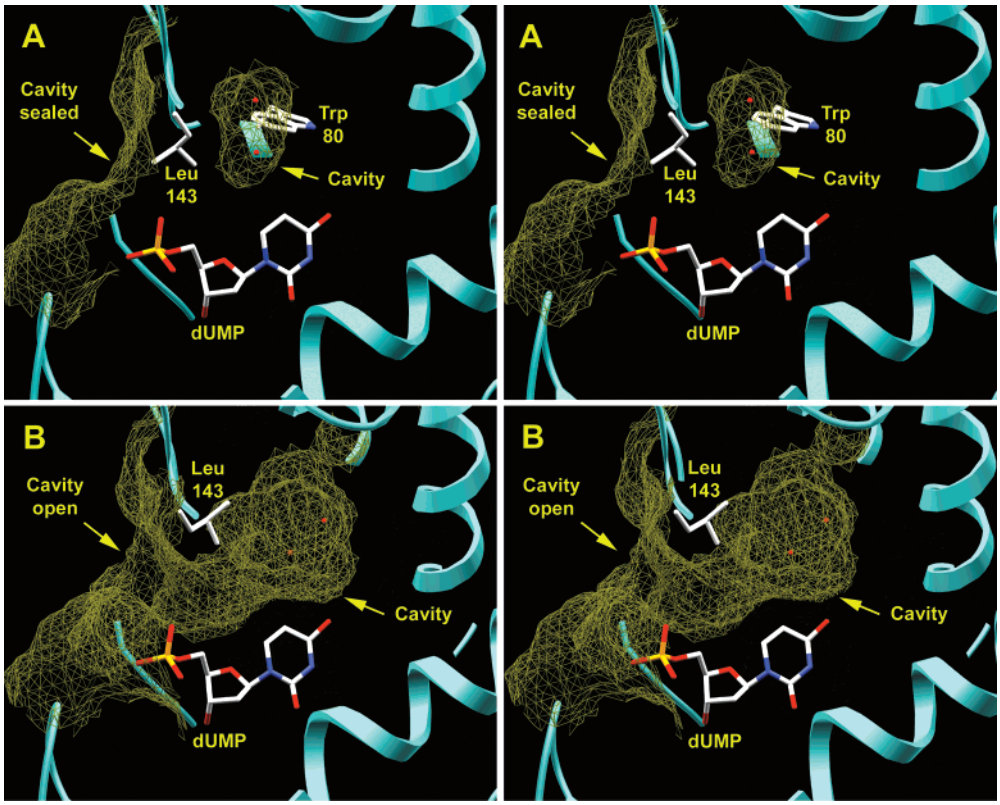

FIGURE 6: Loss of the Trp 80 side chain leads to the expansion of an active site solvent cavity. Panel A shows a divergent stereoview of two water molecules (waters 449 and 524) filling a cavity sealed from bulk solvent in the active site of the wild-type EcTS/dUMP/THF structure. The side chains of Trp 80 and Leu 143 and dUMP are also shown. Panel B shows the same view of the active site of protomer **A** of the W80G-EcTS/dUMP/CB3717 mutant structure. Note the orientation of Leu 143, the enlargement of the active site cavity, and its continuity with bulk solvent. Molecular surfaces of residues lining the active sites were generated using the program Swiss PDB Viewer (*22*) and were used to illustrate the cavity.

does not reorient upon binding CB3717, leaving the cavity exposed to bulk solvent (Figure 6). In the EcTS/dUMP/THF structure, Leu 143 is held in close contact (3.6 Å) with the side chain of Trp 83. The orientation of Leu 143 seen in the W80G-EcTS mutant is prevented in the wild-type structure because of the close contact Leu 143 would form with Trp 80 (3.2 Å) and a conserved active site water molecule (2.7 Å).

DISCUSSION

It has been suggested that the reduction of the dUMP exocyclic methylene by THF occurs as two single-electron transfers rather than a direct transfer of hydride (*7*, *10*). In part, this suggestion is based on model chemical reactions (*25*, *26*) and the observation that the reaction mechanism of amino acid hydroxylases (which require tetrahydropterin) proceed via two single-electron transfers (*27*). However,

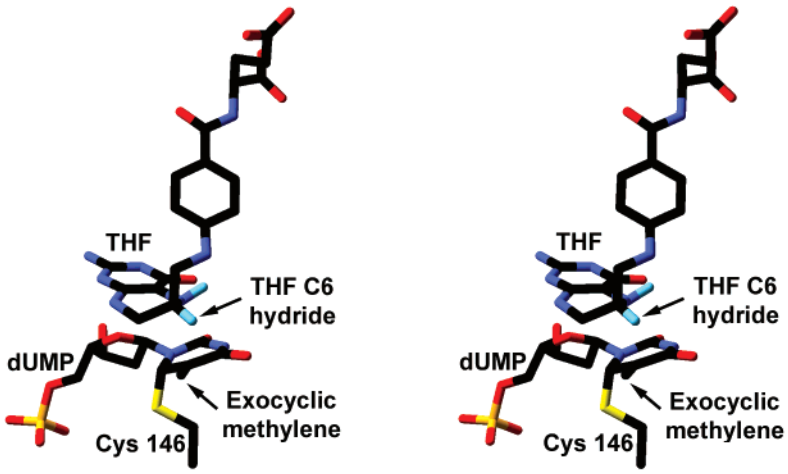

FIGURE 7: THF C6 hydride is optimally positioned for direct donation to the exocyclic methylene. The figure is a divergent stereodiagram of the THF C6 hydride and the dUMP exocyclic methylene modeled in the EcTS/dUMP/THF structure.

model chemical systems are not always reliable predictors of enzyme mechanisms, and the amino acid hydroxylases, unlike TS, use molecular oxygen and require metal ions for activity (*28*). Thus, the mechanism of these enzymes is likely to be different from that of thymidylate synthase.

The "proposed" orientation of THF bound to the active site of EcTS is shown in Figure 3A. This mode of THF binding was based on two observations (*7*). First, the structure of the EcTS/dUMP/BW1843U89 complex (*8*, *9*) suggested that there might be a possible alternative binding site for cofactor. Second, since THF would form a radical cation during the transfer of the first electron from THF to the dUMP exocyclic methylene, this orientation could be stabilized by the π electrons of Trp 80 and stacking interactions with the uracil ring. In this proposal, at the final stage of hydride transfer, THF would shift back into the position normally occupied by cofactor for the donation of the C6 hydrogen atom (final electron and proton).

On the basis of our structure, this scheme for exocyclic methylene reduction seems unlikely. First, the shift of THF from its crystallographically observed position to the proposed alternative site would require breaking four hydrogen bonds between THF and the protein (Figure 4). These hydrogen bonds are between THF N2H and Ala 263 O: a water-mediated hydrogen bond between THF N2H and Ala 263 NH and between THF N3H and Asp 169 Oδ2 and a water-mediated hydrogen bond between THF N1 and Ala 263 O. These disrupted bonds are not reestablished nor are they compensated by new bonds in the proposed structure of THF in the alternative site. Second, THF binding in the alternative site would require some reordering of the protein at energetic cost. THF would come into van der Waals contact with Phe 176 (2.6 Å) and Glu 58 (2.5 Å) and would require reordering of the side chains of these residues. While a reordering of Phe 176 may not present a problem because this residue is seen to adopt alternative conformations depending on the bound ligand (*8*, *9*, *14*), reordering of the Glu 58 side chain would break its hydrogen bond to Trp 80 Nϵ1H. Finally, the shift of THF away from dUMP to the alternative site might break the reversible covalent bond between dUMP and the active site cysteine also, as seen in the EcTS/dUMP/BW1843U89 complex.

The data of Barrett et al., however, in which 15 different substituents were introduced as replacements of Trp 80, provide a good correlation between the value of log(k_{cat}) and the theoretical binding energies of Na^+ binding by the substituted side chains. This could be a long-range electrostatic effect in which the substituents stabilize either a THF carbocation radical formed during a two-step hydride transfer or a cationic transition state formed during direct hydride transfer. Thus, the data support either direct hydride transfer or a two-step hydride transfer mechanism with a carbocation intermediate but without the conformation change to the cofactor that would optimize the radical cation interactions with Trp 80.

It was previously noted that the carbocationic character of the exocyclic methylene should be sufficient to drive hydride transfer given appropriate juxtapositioning of the exocyclic methylene and the THF C6 hydride (*3*). The structure of the EcTS/dUMP/THF complex was used to model the positions of the dUMP exocyclic methylene, the THF C6 hydride, and the THF N5 proton (Figure 7). In the modeled structure, the THF C6 hydride is located only 2.5 Å from the dUMP exocyclic methylene. Furthermore, the modeled structure suggests that during direct hydride transfer, a developing THF N5−C6 double bond would flatten the B ring of the pterin group and would tend to drive the C6 hydride toward the dUMP exocyclic methylene, increasing the opportunity for reaction. However, whether the hydride transfer is direct or occurs by two single-electron transfers cannot be determined from the current crystal structure.

No mutational analyses have been done to address the function of Leu 143 though this residue, as Trp 80, is highly conserved across TS species. The orientation of the Leu 143 side chain in the W80G-EcTS/dUMP/CB3717 structure is unlike that seen in other ternary EcTS complexes but is observed in the apo EcTS (*29*) and the binary EcTS/dUMP (*30*) structures. In the more open apo and binary structures, the $C_\alpha-C_\alpha$ distance between Trp 80 and Leu 143 is 10.8 and 10.9 Å, respectively, versus 10.4 Å in the EcTS/THF/dUMP structure and 10.2 Å in the W80G structure. During segmental accommodation, the protein segments containing Trp 80 and Leu 143 move toward each other as the active site closes around the substrate and cofactor. The orientation of Leu 143 in the W80G structure is made possible by the

mutation of Trp 80, which would otherwise contact Leu 143 in this orientation. It would thus appear that as the active site undergoes segmental accommodation, the side chain of Leu 143 is forced from its initial position to a more external one. The orientation of Leu 143 in the W80G mutant relative to the wild-type enzyme and the resulting bridging of bulk solvent with mutant's cavity may serve to stabilize the enzyme because isolated protein cavities are destabilizing to protein structure (*31*).

Two possible mechanisms for the addition of β-ME to the dUMP exocyclic methylene seem likely. First, the large cavity of the W80G mutant suggests that β-ME may be trapped in the W80G active site and may attack from within the cavity. Indeed, the large cavity volumes of all of the active sites and the closed structure of four of the six W80G active sites suggest an "attack from within" mechanism of HETM-dUMP formation. However, it is possible that β-ME attacks from outside the active site, especially if THF diffuses from the active site after donating the methylene group. One EcTS mutant (V264Am) that produces significant amounts of HETM-dUMP contains the conserved Trp 80 but has the carboxyl terminal Ile 264 removed (*11*). As in the wild-type enzyme, there would not be enough space in the active site of this mutant to accommodate the dUMP exocyclic methylene, THF, and β-ME at the same time, so β-ME must come from the bulk solvent or attack after THF has diffused from the active site. TS carboxyl terminal mutants are deficient in sealing the active site because they lack the carboxylate group of the C-terminus, which forms simultaneous hydrogen bonds to Trp 83, Arg 21, and the cofactor (*32*). This deficiency may allow THF to diffuse from the active site after transferring the methylene group, or it may result in a more open active site in which β-ME can gain access to the dUMP exocyclic methylene in the presence of THF. Determining the mechanism of β-ME addition to the dUMP exocyclic methylene would be aided by the crystal structures of the W80G-EcTS/HETM-dUMP or W80G-EcTS/HETM-dUMP/THF complexes or the corresponding complexes of theV264Am mutant.

Assuming that β-ME is trapped in the active site of the W80G mutant, both THF and β-ME would compete for reaction with the exocyclic methylene. This suggests that β-ME is intrinsically more nucleophilic than THF and/or THF is not optimally positioned for hydride transfer. While the orientation of THF in the W80G mutant remains unknown, two lines of evidence suggest it may not be optimally positioned in the mutant for hydride transfer. First, the Trp 80 side chain forms 39 Å^2 (0.8−1.0 kcal/mol) of hydrophobic contact to THF in the EcTS/dUMP/THF structure. This contact to the protein would be lost in the W80G mutant and replaced by less favorable contact to solvent as suggested by the W80G-EcTS/dUMP/CB3717 structure. Thus, THF would likely be less rigidly held in the active site of the mutant. Indeed, mutation of Trp 82 to Ala in LcTS increases the K_m for mTHF 22-fold, while the K_m for mTHF in the LcTS W82G mutant is undetectable because of the inactivity of the mutant in forming dTMP (*24*). Second, competition between THF and another nucleophile (water) for a pyrimidine exocyclic methylene occurs in the enzyme deoxycytidylate (dCMP) hydroxymethylase. dCMP hydroxymethylase is homologous to TS, and their reactions are very similar. However, instead of reducing the exocyclic methylene with THF, dCMP hydroxymethylase adds water to the exocyclic methylene, producing 5-hydroxymethyl-dCMP and THF. dCMP hydroxymethylase is 27 residues shorter than EcTS. Several of these EcTS C-terminal residues (Ile 258, Ala 260, Val 262, and Ala 263) serve to stabilize mTHF (and THF) in the active site (Figure 4). These interactions are not possible in dCMP hydroxymethylase, and as a result, the orientation of THF in the dCMP hydroxymethylase active site may differ from that of THF in the EcTS active site. The crystal structure of dCMP hydroxymethylase has been determined but contains no cofactor, so the orientation of THF (or mTHF) in the active site remains unknown (*33*).

The structures of apo EcTS (*29*) and EcTS bound to dUMP alone (*30*), to dUMP and mTHF (*23*, *34*), and to the products dTMP and 7,8-dihydrofolate (*35*) have provided a wealth of information complementing the biochemical data of the TS reaction mechanism (*2*, *3*). This paper presents information on the structure of TS at the rate-limiting step of its reaction mechanism, the hydride transfer step. Our structure shows that THF is ideally oriented to reduce the exocyclic methylene without changing its active site location as previously proposed (*7*). Thus, the structure of dUMP and THF bound to EcTS presented in this paper fills one of the last remaining gaps in the structural knowledge of the various stages of the TS reaction mechanism.

ACKNOWLEDGMENT

The authors thank Eprova AG, Switzerland, for the gift of mTHF and THF. We also thank Wallace Cleland and Drs. Julian Chen and Kinkead Reiling for helpful discussions.

REFERENCES

1. Spencer, H. T., Villafranca, J. E., and Appleman, J. R. (1997) *Biochemistry 36*, 4212−4222.
2. Stroud, R. M., and Finer-Moore, J. S. (1993) *FASEB J. 7*, 671−677.
3. Carreras, C. W., and Santi, D. V. (1995) *Annu. Rev. Biochem. 64*, 721−762.
4. Montfort, W. R., Perry, K. M., Fauman, E. B., Finer-Moore, J. S., Maley, G. F., Hardy, L., Maley, F., and Stroud, R. M. (1990) *Biochemistry 29*, 6964−6977.
5. Liu, Y., Barrett, J. E., Schultz, P. G., and Santi, D. V. (1999) *Biochemistry 38*, 848−852.
6. Barrett, J. E., Maltby, D. A., Santi, D. V., and Schultz, P. G. (1998) *J. Am. Chem. Soc. 120*, 449−450.
7. Barrett, J. E., Lucero, C. M., and Schultz, P. G. (1999) *J. Am. Chem. Soc. 121*, 7965−7966.
8. Stout, T. J., and Stroud, R. M. (1996) *Structure 4*, 67−77.
9. Weichsel, A., and Montfort, W. R. (1995) *Nat. Struct. Biol. 2*, 1095−101.
10. Slieker, L. J., and Benkovic, S. J. (1984) *J. Am. Chem. Soc. 106*, 1833−1838.
11. Variath, P., Liu, Y., Lee, T. T., Stroud, R. M., and Santi, D. V. (2000) *Biochemistry 39*, 2429−2435.
12. Maley, G. F., and Maley, F. (1988) *J. Biol. Chem. 263*, 7620−7627.
13. Otwinowski, Z., and Minor, W. (1997) *Methods Enzymol. 276*, 307−326.
14. Rutenber, E. E., and Stroud, R. M. (1996) *Structure 4*, 1317−1324.
15. Navaza, J. (1994) *Acta Crystallogr., Sect. A 50*, 157−163.
16. Kissinger, C. R., Gehlhaar, D. K., and Fogel, D. B. (1999) *Acta Crystallogr., Sect. D 55*, 484−491.
17. McRee, D. E. (1999) *J. Struct. Biol. 125*, 156−165.

18. Brünger, A. T., Adams, P. D., Clore, G. M., DeLano, W. L., Gros, P., Grosse-Kunstleve, R. W., Jiang, J. S., Kuszewski, J., Nilges, M., Pannu, N. S., Read, R. J., Rice, L. M., Simonson, T., and Warren, G. L. (1998) *Acta Crystallogr., Sect. D 54*, 905−921.
19. Kleywegt, G. J., and Jones, T. A. (1994) *Acta Crystallogr., Sect. D 50*, 178−185.
20. Wallace, A. C., Laskowski, R. A., and Thornton, J. M. (1995) *Protein Eng. 8*, 127−134.
21. Sobolev, V., Sorokine, A., Prilusky, J., Abola, E. E., and Edelman, M. (1999) *Bioinformatics 15*, 327−332.
22. Guex, N., and Peitsch, M. C. (1997) *Electrophoresis 18*, 2714−2723.
23. Hyatt, D. C., Maley, F., and Montfort, W. R. (1997) *Biochemistry 36*, 4585−4594.
24. Kealey, J. T., Eckstein, J., and Santi, D. V. (1995) *Chem. Biol. 2*, 609−614.
25. Meissner, J. W. G., and Pandit, U. K. (1992) *Tetrahedron Lett. V33*, 2999−3002.
26. Ehrenberg, A., Hemmerich, P., Muller, F., Okada, T., and Viscontini, M. (1967) *Helv. Chim. Acta 50*, 411−416.
27. Kaufman, S. J. (1961) *J. Biol. Chem. 236*, 804−810.
28. Fitzpatrick, P. F. (1999) *Annu. Rev. Biochem. 68*, 355−381.
29. Perry, K. M., Fauman, E. B., Finer-Moore, J. S., Montfort, W. R., Maley, G. F., Maley, F., and Stroud, R. M. (1990) *Proteins 8*, 315−333.
30. Stout, T. J., Sage, C. R., and Stroud, R. M. (1998) *Structure 6*, 839−848.
31. Eriksson, A. E., Baase, W. A., Zhang, X. J., Heinz, D. W., Blaber, M., Baldwin, E. P., and Matthews, B. W. (1992) *Science 255*, 178−183.
32. Perry, K. M., Carreras, C. W., Chang, L. C., Santi, D. V., and Stroud, R. M. (1993) *Biochemistry 32*, 7116−7125.
33. Song, H. K., Sohn, S. H., and Suh, S. W. (1999) *EMBO J. 18*, 1104−1113.
34. Matthews, D. A., Villafranca, J. E., Janson, C. A., Smith, W. W., Welsh, K., and Freer, S. (1990) *J. Mol. Biol. 214*, 937−948.
35. Fauman, E. B., Rutenber, E. E., Maley, G. F., Maley, F., and Stroud, R. M. (1994) *Biochemistry 33*, 1502−1511.
36. Kleywegt, G. J. (1996) *Acta Crystallogr., Sect. D 52*, 842−857.

BI012108C